# Dermatan sulfate epimerase 2 is the predominant isozyme in the formation of the chondroitin sulfate/dermatan sulfate hybrid structure in postnatal developing mouse brain

**Chizuru Akatsu[2,4], Shuji Mizumoto[2], Tomoyuki Kaneiwa[2], Marco Maccarana[3], Anders Malmström[3], Shuhei Yamada[1, 2], and Kazuyuki Sugahara[1, 2]**

[2]Laboratory of Proteoglycan Signaling and Therapeutics, Hokkaido University Graduate School of Life Science, Sapporo 001-0021, Japan

[3]Department of Experimental Medical Science, Biomedical Center D12, Lund University, SE-221 84 Lund, Sweden

[1]To whom correspondence should be addressed: Tel: 81-11-706-9054; Fax: 81-11-706-9056; e-mail: k-sugar@sci.hokudai.ac.jp, and Tel: 81-11-706-9055; Fax: 81-11-706-9055; e-mail: tjohej@sci.hokudai.ac.jp

**Running title**: Dermatan sulfate epimerases in the developing mouse brain

**Key words:** Brain development/Chondroitin sulfate/Dermatan sulfate/Dermatan sulfate epimerase/Proteoglycan

**Abstract**

Chondroitin sulfate (CS) and dermatan sulfate (DS) are expressed in significant amounts in the brain and play important roles in the development of the central nervous system in mammals. CS and DS structures are often found in a single CS/DS hybrid chain. The L-iduronic acid (IdoA)-containing domain, which defines a DS-type domain, appears key to the biological functions of the CS/DS hybrid chain. In this study, to clarify the distribution of the DS-type structure in the brain during development, the expression patterns of DS epimerase 1 (DS-epi1) and DS-epi2, both of which convert D-glucuronic acid (GlcA) into IdoA, were investigated by *in situ* hybridization. *DS-epi2* was ubiquitously expressed in the developing brain after birth, whereas the expression of *DS-epi1* was faint and obscure at all developmental stages. Quantitative real-time PCR revealed the expression of *DS-epi2* to be higher than that of *DS-epi1* throughout development, suggesting that DS-epi2 but not DS-epi1 is mostly expressed in the brain and plays key roles in the epimerization of CS/DS during its biosynthesis. Moreover, an analysis of the disaccharides of CS/DS demonstrated significant amounts of IdoA-containing iD units [IdoA(2S)-GalNAc(6S)] and iB units [IdoA(2S)-GalNAc(4S)], where 2S, 4S, and 6S stand for 2-*O*-, 4-*O*-, and 6-*O*-sulfate, respectively, in every region of the brain examined. The proportion of these units in cerebellar CS/DS was greatly altered during postnatal development. These results suggest that the IdoA-containing structures in the developing brain are mainly produced by the actions of

DS-epi2 and play crucial roles in the postnatal development.

## Introduction

Chondroitin sulfate (CS) and dermatan sulfate (DS) are sulfated glycosaminoglycans (GAGs), which are linear polysaccharides covalently bound to serine residues of specific core proteins forming proteoglycans (PGs). CS and DS are composed of repeating disaccharide units, GlcA-GalNAc and IdoA-GalNAc (Fig. 1), where GlcA, IdoA, and GalNAc represent D-glucuronic acid, L-iduronic acid, and *N*-acetyl-D-galactosamine, respectively. DS is a stereoisomeric variant of CS containing IdoA instead of GlcA residues, and CS and DS are often found in a single polysaccharide chain as a CS/DS hybrid structure (Habuchi et al. 1973; Sugahara and Mikami 2007). The IdoA-containing disaccharides can be adjacent, forming long blocks, or singly interspersed among GlcA-containing disaccharides (Pacheco et al. 2009b). The simple disaccharide backbone of CS/DS is modified most notably by sulfation at various positions to form a variety of disaccharide units as shown in Fig. 1. The combination of these various units provides CS/DS with enormous structural heterogeneity along its length.

CS/DS is mainly distributed in extracellular matrices and at cell surfaces, and plays an important role in many biological functions under physiological and pathological conditions. Accumulating evidence has demonstrated that CS/DS regulates biological processes by interacting with and regulating various functional protein ligands such as growth factors, neurotrophic factors, and cytokines (Sugahara and Mikami, 2007; Yamada and Sugahara

2008). CS/DS binds to bioactive proteins through oligosaccharide domains composed of specific disaccharide sequences, which may hence greatly influence the functions of CS/DS. Highly-sulfated CS chains containing D units [GlcA(2S)-GalNAc(6S)] or E units [GlcA-GalNAc(4S,6S)] show neuritogenic activity (Nadanaka et al. 1998; Clement et al. 1999). Defective 6-*O*-sulfation of CS causes chondrodysplasia and skeletal dysplasia (Thiele et al. 2004; van Roij et al. 2008; Tuysuz et al. 2009). The specific sulfation patterns in CS/DS chains appear to be critical to their functions. Studies have shown that IdoA residues are also key factors in the formation of such functional domains. Some bioactive proteins including heparin cofactor II, fibroblast growth factor (FGF)-2, FGF-7, and pleiotrophin require IdoA-containing domains for interaction with CS/DS (Maimone and Tollefsen 1990; Penc et al. 1998; Trowbridge et al. 2002; Bao et al. 2005).

Recent studies using rodents have demonstrated that thousands of fresh neurons arise even in the adult brain every day particularly in the hippocampus, a structure involved in learning and memory (Shors 2009). However, little is known about the molecular basis. CS/DS chains are implicated in the development of the central nervous system in mammals, in which IdoA residues appear to play important roles. The CS/DS hybrid moieties of a DSD-1-PG isolated from neonatal mouse brain (Faissner et al. 1994) showed neuritogenic activity toward hippocampal neurons *in vitro* (Clement et al. 1998). Highly-sulfated DS polysaccharides purified from various marine organisms also exhibited neuritogenic activity

(Hikino et al. 2003; Nandini et al. 2004, 2005; Li et al. 2007, 2010). In addition, CS/DS hybrid chains purified from embryonic pig brains, which displayed remarkable neuritogenic activity, contained a higher proportion of IdoA than those from adult brains, which showed little neuritogenic activity (Bao et al. 2004). These results indicate that the DS-type structure exists in the brain and is involved in neuritogenesis. Furthermore, it has recently been reported that IdoA-containing CS/DS chains are concentrated in the elaborating cerebellum after birth, where the cerebellar system is dramatically matured (Mitsunaga et al. 2006), suggesting the DS-type structure to be involved in the brain's development *in vivo*.

During the biosynthesis of CS/DS, the polysaccharide backbone of chondroitin composed of alternating GlcA and GalNAc units is constructed first (Kitagawa et al. 2001, 2003). The structural diversity of CS/DS is generated by ensuing modifications such as C5-epimerization and *O*-sulfation under the control of two DS epimerases (DS-epi1 and DS-epi2), which convert GlcA into IdoA (Maccarana et al. 2006; Pacheco et al. 2009b), and distinct sulfotransferases (Kusche-Gullberg and Kjellén 2003), respectively. *O*-Sulfation, which takes place after the C5-epimerization, has been postulated to be involved in the fixation of DS-type structures by preventing back epimerization reactions (Malmström 1984). Dermatan 4-*O*-sulfotransferase-1 (D4ST-1) and uronyl 2-*O*-sulfotransferase (UST) are responsible for the 4-*O*-sulfation of GalNAc and 2-*O*-sulfation of IdoA residues in DS chains, respectively, to form iA units [IdoA-GalNAc(4S)] and iB units [IdoA(2S)-GalNAc(4S)]

(Kobayashi et al. 1999; Mikami et al. 2003).

Previously, the expression level of both *D4ST-1* and *UST* was demonstrated to be higher in cerebellum than in whole brain during postnatal development (Mitsunaga et al. 2006). Further, the accumulation of IdoA-containing structures in cerebellum has been observed. Although C5-epimerization is a rate-limiting step in the biosynthesis of DS, the respective expression of *DS-epi1* and *DS-epi2* in mouse brain during postnatal development remains to be elucidated. The recently cloned DS-epi1 (coded by the gene *Dse*) and DS-epi2 (coded by *Dse-like* (*Dsel*)) share a highly conserved ~700 amino acid domain of active epimerase (Maccarana et al. 2006; Pacheco et al. 2009b). In addition, DS-epi2 has a C-terminal domain similar to CS/DS-sulfotransferase (Goossens et al. 2003; Pacheco et al. 2009b), although its activity remains to be established. In this study, the expression pattern of *DS-epi1* and *DS-epi2*, as well as the structure of CS/DS from the brain during postnatal development, were investigated to gain insights into the distribution and function of the IdoA-containing structures.

## Results

*Expression of DS-epi1 and DS-epi2 in the mouse brain during postnatal development*

The formation of IdoA by C5-epimerization of GlcA is the initial modification of the CS/DS hybrid chain (Malmström 1984), and catalyzed by two C5-epimerases DS-epi1 and DS-epi2

encoded by *Dse* and *Dsel* genes, repectively (Maccarana et al. 2006; Pacheco et al. 2009b). It has been reported that IdoA-containing structures in CS/DS hybrid chains are important for neuritogenic activity (Sugahara and Mikami 2007) and postnatal development of the brain, especially cerebellum (Mitsunaga et al. 2006; Ishii and Maeda 2008).

To investigate the distribution and function of such structures, the expression patterns of the *DS-epi1* and *DS-epi2* transcripts were examined by *in situ* hybridization using $^{35}$S-labeled antisense probes in sagittal sections prepared from mouse brains at postnatal day (P) 7, P14, P21, and 7 weeks (7W) (Fig. 2). The *DS-epi2* transcript was detected in widespread regions including the olfactory bulb, caudate putamen, cerebral cortex, hippocampus, thalamus, midbrain, and cerebellum (Figs. 2, *A*-*D*). In the negative control experiments with the respective $^{35}$S-labeled sense probe, essentially no signal was detected in the sections of P21 (Fig. 2*E*), P7, P14, or 7W (data not shown) mice, confirming the specific hybridization of the antisense probe. The widespread expression of *DS-epi2* seen at P7 and P14 was more restricted at P21 and 7W. As shown in Figs. 2*A* and 2*B*, *DS-epi2* was expressed ubiquitously in the mouse brain but its expression was marked in the hippocampus and thalamus in P7 and P14 mice. On the other hand, intense labeling of *DS-epi2* was restricted to the hippocampus, thalamus, and cerebral cortex in the brains of P21 and 7W mice (Fig. 2*C* and 2*D*), indicating that the expression pattern of *DS-epi2* in mouse brain changed with postnatal development. In contrast, almost no *DS-epi1* was detected at P21 (Fig. 2*F*), or at any other stage (data not

shown). These results suggest the expression of *DS-epi1* to be much lower than that of *DS-epi2* in every region and at every stage examined.

The detailed expression pattern of *DS-epi2* was further investigated by microautoradiographic analysis (Fig. 3) in the brain section of 7W mice, where intense signals of *DS-epi2* were observed in the hippocampus, thalamus, and cerebral cortex by film autoradiography (Fig. 2*D*). To identify the cell types expressing *DS-epi2*, the granule cell layer of the dentate gyrus was counterstained with cresyl violet (Nissl stain) for comparison. The higher magnification views showed that the signal of the *DS-epi2* transcript was detected in the hippocampus (Fig. 3*A* and 3*C*), thalamus, and caudate putamen (data not shown). In the hippocampus, the predominant signal was observed in the pyramidal cell layer of the CA1-CA3 fields (Fig. 3*A*). Although prominent signals of *DS-epi2* were also observed in the thalamus and caudate putamen, the cell types expressing *DS-epi2* could be hardly identified due to the weak counterstaining by cresyl violet (data not shown).

Consistent with the findings obtained by *in situ* hybridization (Fig. 2), quantitative real-time PCR revealed higher levels of *DS-epi2* than *DS-epi1* in the olfactory bulb, cerebrum/midbrain, cerebellum, and pons/medulla oblongata at all developmental stages (Fig. 4). The expression of *DS-epi1* showed only moderate changes during development, whereas that of *DS-epi2* fluctuated greatly. As shown in Fig. 4B, in cerebrum/midbrain, the highest level of *DS-epi2* was observed at P7. The expression of *DS-epi2* dropped to a low level at P14,

subsequently increased at P21, and then decreased a little at 7W. Similar fluctuations in the expression of *DS-epi2* during postnatal development were observed in the other three regions (Figs. 4*A*, 4*C*, and 4*D*). At P7 the expression was higher in cerebrum/midbrain and cerebellum than in the olfactory bulb and pons/medulla oblongata. These findings suggest that DS-epi2, but not DS-epi1, is expressed in mouse brain during the development of the central nervous system, and plays a predominant role in the biosynthesis of the IdoA-containing structures in CS/DS hybrid chains.

*Compositional change of CS/DS disaccharides in various regions of the brain during postnatal development*

To assess the regional distribution of IdoA-containing units in CS/DS hybrid chains from various regions of the brain in the postnatal period, the disaccharide composition of CS/DS was determined using specific CS/DS-degrading enzymes. GAG-peptide fractions were individually prepared from the olfactory bulb, cerebrum/midbrain, cerebellum, and pons/medulla oblongata of P7, P14, P21, and 7W mice, and an aliquot was digested with chondroitinase (CSase) ABC alone or a mixture of CSases AC-I and AC-II, and subsequently derivatized with a fluorophore, 2-aminobenzamide (2AB). It should be noted that the digestion with CSase ABC was carried out in the buffer mentioned under “Materials and methods” instead of the conventional buffer (50 mM Tris-HCl buffer, pH 8.0, containing 60

mM sodium acetate), so that the efficacy of the 2AB-derivatization of CSase ABC digests would be comparable to that of the digests using a mixture of CSases AC-I and AC-II (Mitsunaga et al. 2006). The 2AB-derivatives of the CS/DS disaccharides were subjected to anion-exchange HPLC and quantified based on the fluorescence intensity of their peaks. The unsaturated disaccharides of CS/DS were identified by comparison with the elution positions of authentic 2AB-labeled disaccharides. Note that CSase ABC cleaves the *N*-acetylgalactosamidic bonds adjacent to not only GlcA but also to IdoA ([-3GalNAcβ1-4GlcAβ1-] and [-3GalNAcβ1-4IdoAα1-]) in both CS and DS, whereas CSases AC-I and AC-II cleave the bond flanked only by GlcA ([-3GalNAcβ1-4GlcAβ1-]) in CS (Petit et al. 2006). Hence, the linkage sensitive to CSase ABC but resistant to CSases AC-I and AC-II can be estimated to be the IdoA-containing structure in CS/DS chains (Habuchi et al. 1973), and the amount of IdoA-containing disaccharide was calculated as follows: the total amount of disaccharides released by digestion with CSase ABC minus that released by digestion with a mixture of CSases AC-I and AC-II. Although it has been reported that the galactosaminidic linkage adjacent to 2-*O*-sulfated GlcA [-3GalNAcβ1-4GlcA(2S)β1-] is also resistant to CSases AC-I and AC-II (Yoshida et al. 1993), a recent study has demonstrated that it is cleavable by CSase AC-II under harsh conditions (Ohtake et al. 2003).

Representative chromatograms of the digests of CS/DS derived from cerebrum/midbrain with CSase ABC or CSases AC-I and AC-II are shown in Fig. 5. Similar

chromatograms were obtained from other regions (data not shown). The disaccharide composition detected by anion-exchange HPLC is summarized in Fig. 6. The CS/DS preparations from olfactory bulb, cerebrum/midbrain, cerebellum, and pons/medulla oblongata mainly contained mono- and nonsulfated disaccharide units (Figs. 6*A*, 6*C*, 6*E*, and 6*G*). The major disaccharide unit in the CS/DS preparations was always the A unit, followed by the C and O units. Although a minute amount of iA was detected, no iC and iO was observed. During the development of all regions of the brain, the proportion of A unit increased, whereas that of C and O units decreased. This developmental change in the sulfation pattern of CS/DS chains was also observed during embryonic development in the chick (Kitagawa et al. 1997).

Since a strong signal of the *DS-epi2* transcript was observed in the thalamus of a 7W mouse brain (Fig. 2D), the disaccharide composition of CS/DS in the thalamus was analyzed and compared with that in the cerebral cortex of a 7W mouse brain (Supplementary Table I). Although iD and iB units in the cortex were approximately one third of those in the thalamus, the small difference in the ratio of DS disaccharides to CS disaccharides does not appear to be significant, suggesting that the DS-epi2 may not play the critical role in the construction of the IdoA-containing structure but rather the sulfotransferases may mainly contribute to the DS biosynthesis in the brain as discussed later.

The total amount of CS/DS disaccharides in all regions examined decreased with

postnatal development. CS/DS in the cerebrum/midbrain and pons/medulla oblongata decreased more drastically during development (Figs. 6*C* and 6*G*) than in the olfactory bulb and cerebellum (Figs. 6*A* and 6*E*).

The amounts of disulfated disaccharides, D, iD, B, iB, E, and iE units, in CS/DS chains from various regions of the mouse brain were much less than those of mono- and nonsulfated disaccharides, A, C, and O units. However, they were significantly present throughout the postnatal development in small amounts (Figs. 6*B*, 6*D*, 6*F*, and 6*H*). Since evidence for the biological significance of such highly sulfated disaccharides has been accumulated (Yamada and Sugahara 2008; Li et al. 2008; Basappa et al. 2009), determination of the temporal change in their amounts and proportions is also important. The proportion of iE units was very small compared to that of iB or iD units in CS/DS from all regions of the mouse brain. It should be noted that the amounts of iD and iB units detected may be slightly overestimated because the galactosaminidic linkages adjacent to B and D units containing a 2-*O*-sulfated GlcA residue are less sensitive to a mixture of CSases AC-I and AC-II as mentioned above, and because B and D units in the tetrasaccharide sequences such as B-iA and D-iA are not released as disaccharides by digestion with CSase AC-I or AC-II. The relative proportions of disulfated disaccharides of CS/DS in the olfactory bulb, cerebrum/midbrain, and pons/medulla oblongata were relatively constant during postnatal development (Figs. 6*B*, 6*D*, and 6*H*), although the total amount of CS/DS in the cerebrum/midbrain and pons/medulla oblongata

was significantly reduced (Figs. 6C, 6*D*, 6*G*, and 6*H*). On the opposite, a drastic change in the proportions of disulfated disaccharides in cerebellar CS/DS preparations was observed (Fig. 6*F*). During P14 to P21 in the cerebellum, the proportion of iD units decreased by half (Fig. 6*F*, *light gray*), whereas that of iB units increased more than four fold (Fig. 6*F*, *light blue*). The proportions of D and E units were slightly reduced in this region during development (Fig. 6*F*, *dark gray* and *pink*, respectively). Since the cerebellar system dramatically grows after birth, the marked increase in the proportion of IdoA-containing disaccharides in cerebellum CS/DS may be correlated with the postnatal development of the cerebellum as discussed later.

In this study, the ΔB unit was detected in the CSase AC-I and AC-II digests (Figs. 5 and 6), being most likely derived from the B unit not iB unit. The B unit has been detected in shark skin CS/DS (Nandini et al. 2005), but never in mammalian tissues. Thus, the presence of the B unit in mammals was reported here for the first time.

**Discussion**

DS-epimerases convert GlcA to IdoA by catalyzing the C5-epimerization of GlcA residues, which is the initial modifying step in the biosynthesis of IdoA-containing structures in CS/DS. Two DS-epimerases, DS-epi1 and DS-epi2, coded by the *Dse* and *Dsel* genes, respectively, have been identified and characterized (Maccarana et al. 2006; Pacheco et al. 2009b). *DS-epi1*

is ubiquitously expressed in vertebrates and at high levels in certain cancer cells (Nakao et al. 2000). *DS-epi2* is also ubiquitously expressed in vertebrates but its highest expression has been shown in the brain where low levels of *DS-epi1* have been observed (Goossens et al. 2003). This was in good agreement with results of an analysis of DS-epi1-deficient mice (Maccarana et al. 2009). The epimerase activity in spleen, kidney, lung, and skin from DS-epi1-deficient mice was less than 35% of that of the corresponding organs of wild-type mice, whereas 86% of the epimerase activity remained in the brain of the homozygous mouse compared with the wild-type. *DSEL* (*DS-epi2*) was originally identified as *C18orf4*, which was genetically associated with manic-depressive disorders (Goossens et al. 2003), suggesting an indispensable role for DS-epi2 in the brain. In the present study, the expression of *DS-epi2* was investigated in various regions of the brain; olfactory bulb, cerebrum/midbrain, cerebellum, and pons/medulla oblongata, and demonstrated to be higher than that of *DS-epi1* in every developmental stage examined (Figs. 2 and 4), indicating that DS-epi2 but not DS-epi1 plays a predominant role in the biosynthesis of IdoA-containing CS/DS structures in the brain.

Two IdoA-containing domains are present in a CS/DS hybrid chain (Fransson and Rodén 1967; Habuchi et al. 1973; Cöster et al. 1975; Sugahara and Mikami 2007); an “IdoA block” in which IdoA residues are clustered to form a $[\text{IdoA-GalNAc(4S)}]_{n \geq 4}$ structure, and a “hybrid structure” where an IdoA residue or a few clustered IdoA residues alternate with GlcA

residues. In this study, the disaccharide composition of CS/DS in various brain regions during postnatal development was investigated. CS/DS chains expressed in the brain contained a larger proportion of GlcA and a smaller proportion of IdoA, mainly being observed as disulfated disaccharides, iB and iD units (Figs. 5 and 6). Although disulfated disaccharide units have been demonstrated in CS/DS hybrid chains (Sugahara and Mikami 2007), few were detected in the digests of GAG-peptide preparations obtained using CSase B (data not shown), which specifically acts on the galactosaminidic bond in the [-3GalNAcβ1-4IdoAα1-] sequence (Michelacci and Dietrich 1974), suggesting that such disulfated disaccharides form the hybrid CS/DS structure in mouse brain and that long “IdoA blocks”, detected as iA, were a minor component.

Although *DS-epi2* is widely expressed in the brain (Figs. 2 and 4), IdoA-containing structures were more concentrated in the cerebellum than in other regions examined (Fig. 6), consistent with a previous report (Mitsunaga et al. 2006). The ratio of DS to CS in the GAG preparation from the thalamus of a 7W mouse brain, where *DS-epi2* is highly expressed, was not significantly higher than that from other regions in the mouse brain (Supplementary Table I). These findings may be due to the expression of the sulfotransferases catalyzing *O*-sulfation subsequent to C5-epimerization. In the biosynthesis of iB units, GalNAc-4-*O*-sulfation takes place immediately after C5-epimerization of GlcA resulting in production of the iA unit by D4ST-1, which mainly contributes to the 4-*O*-sulfation of GalNAc adjacent to IdoA (Mikami

et al. 2003). UST, then, efficiently catalyzes the 2-*O*-sulfation of the IdoA residue of iA, forming the iB unit (Kobayashi et al. 1999). The preferential expression of *D4ST-1* and *UST* in the cerebellum during postnatal development has been reported (Mitsunaga et al. 2006; Ishii and Maeda 2008), suggesting a positive correlation with the relatively large proportion of iB units in cerebellar CS/DS chains compared to other regions (Fig. 6). D4ST-1 and/or UST might be a rate-limiting factor for the formation of IdoA-containing disaccharide units. The 4-*O*-sulfation is believed to prevent the epimerization of newly formed IdoA back into GlcA (Malmström 1984). In fact, the knockdown of *D4ST-1* led to a significant reduction in IdoA residues (Pacheco et al. 2009a). Since the presence of iO units has not been clearly demonstrated so far for any animals, *O*-sulfation may be required for the fixation of DS-type disaccharides. Recently we and others have discovered new types of human Ehlers-Danlos syndrome with D4ST-1 deficiency, where DS in skin fibroblasts of the patients is completely replaced by CS (Dündar et al. 2009; Miyake et al. 2010). No 4-*O*-sulfation of GalNAc resdiues most likely cannot prevent the epimerization of newly formed IdoA back into GlcA. Interestingly, the decorin proteoglycan with a CS chain but without a DS chain of the patient was shown, which possibly leads to decreased flexibility of collagen bundles (Miyake et al. 2010), manifesting the characteristic symptoms including joint and skin laxity and tissue fragility.

Although the IdoA-containing disulfated disaccharides, iB and iD units, were observed

during embryonic development of the mouse brain, their respective precursors, iA and iC units, were hardly detected (Fig. 6). The 2-*O*-sulfation of IdoA might have occurred prior to or almost simultaneously with the 4-*O*- or 6-*O*-sulfation of GalNAc. UST can also transfer sulfate groups to IdoA residues adjacent to nonsulfated GalNAc residues (Kobayashi et al. 1999). *O*-Sulfotransferases involved in the biosynthesis of CS/DS might interact with each other and co-localize in the Golgi lumen. Enzymes of GAG biosynthesis are believed to work as complexes, to facilitate the transfer of the polysaccharide substrate from one enzyme to the following one efficiently (Esko and Selleck 2002). In fact, physical interactions between pairs of biosynthetic enzymes of heparan sulfate have been shown to influence their enzymatic activities (McCormick et al. 2000; Senay et al. 2000; Pinhal et al. 2001; Presto et al. 2008). In CS biosynthesis, it has been also demonstrated that chondroitin's polymerization is accomplished by multiple combinations of chondroitin synthase-1 (ChSy-1), ChSy-2, ChSy-3, and chondroitin-polymerizing factor (Kitagawa et al. 2003; Izumikawa et al. 2007, 2008). Although no direct interaction has been detected between D4ST-1 and either or both of the DS-epimerases in overexpression experiments (Pacheco et al. 2009a), the possibility cannot be excluded that other enzymes or components associate with them to form a large enzyme complex.

The total amount of CS/DS per mg of acetone powder in every brain region examined decreased during postnatal development (Fig. 6). The reduction in the cerebrum/midbrain and

pons/medulla oblongata was more drastic (Figs. 6*C* and 6*G*) than that in the olfactory bulb and cerebellum (Figs. 6*A* and 6*E*). This observation might be closely correlated with the maturation of the brain. The former regions grow during embryonic development, whereas the latter develop dramatically after birth (Rodier 1977). The minute reduction in the amount of CS/DS in the olfactory bulb and cerebellum with postnatal development may reflect the importance of CS/DS in the postnatal development of the brain. Furthermore, the sulfation profiles of CS/DS chains derived from every region changed with postnatal development (Fig. 6). Notably, marked temporal changes, an increase in iB units and a decrease in iD units, were observed in the cerebellum (Fig. 6*F*). Although the exact biological significance of the developmental changes in the sulfation profile is still unclear, it is possible that they affect the ability of CS/DS chains to interact with functional proteins.

IdoA-containing disulfated disaccharides were present at significant levels in every region examined in this study (Fig. 6), and DS-epi2 seems to predominantly contribute to the biosynthesis of such disaccharide units in the mouse brain (Fig. 4). The structural functions of IdoA include giving flexibility of CS/DS chains, providing substantial conformational diversity, and facilitating the interaction of the sugar chains with proteins (Casu et al. 1988; Ferro et al. 1990). A large number of functional proteins require IdoA-containing structures in CS/DS chains for their binding (Maimone and Tollefsen 1990; Penc et al. 1998; Trowbridge et al. 2002; Bao et al. 2005; Li et al. 2007). However, it remains to be investigated how the

IdoA-containing disulfated disaccharides regulate the functions of these proteins, which are involved in the development and maturation of the brain.

## Materials and methods

### *Materials*

The following sugars and enzymes were purchased from Seikagaku Corp. (Tokyo, Japan): six authentic unsaturated CS disaccharides, ΔHexAα1-3GalNAc (ΔO), ΔHexAα1-3GalNAc(6S) (ΔC), ΔHexAα1-3GalNAc(4S) (ΔA), ΔHexA(2S)α1-3GalNAc(6S) (ΔD), ΔHexA(2S)α1-3GalNAc(4S) (ΔB), and ΔHexAα1-3GalNAc(4S,6S) (ΔE); CSase ABC (EC 4.2.2.20) from *Proteus vulgaris*, CSase AC-I (EC 4.2.2.5) from *Flavobacterium heparinum*, and CSase AC-II (EC 4.2.2.5) from *Arthrobacter aurescens*. ddY Mice at postnatal day P7, P14, P21, and 7W were purchased from SLC Inc. (Shizuoka, Japan).

### *Cloning of mouse cDNA encoding DS-epi1 and DS-epi2*

Single stranded cDNA was synthesized by reverse transcription using total RNA from normal murine mammary gland epithelial (NMuMG) cells obtained from American Type Culture Collection (Manassas, VA). The full-length open reading frames encoding *DS-epi1* and *DS-epi2* were amplified from the cDNA by two rounds of PCR using specific primers corresponding to the sequences in the 5'- and 3'-noncoding regions. A cDNA fragment (~3.1

kbp) encoding mouse *DS-epi1* (GenBank acc. number, NM_172508, also known as *Dse*), was prepared by PCR with the forward primer (F) 5'-GAG GAC GGA GCG GAT CAT TCG AA-3' and the reverse primer (R) 5'-CCT AGG TAC ATC CTT TGT GTG TC-3', followed by nested PCR with F 5'-GAT TTG GCT GCC TTG GAG ACT-3' and R 5'-GCT CAA GTA AAT CTG GAC GAG-3'. A cDNA fragment (~4.0 kbp) encoding mouse *DS-epi2* (NM_001081316, also known as *Dse-like*) was generated by PCR with F 5'-GCT GAA TGT CAC CTG GAT TTC AC-3' and R 5'-TGC TAG GCC AAA TAT GGT GCC TA -3', followed by nested PCR with F 5'-GGA AAC ACT GTG CTT AAC ACA-3' and R 5'-TAG GTT GGG ACA CAT TAG TGC-3'. Each PCR was carried out with *KOD*-Plus DNA polymerase (Toyobo, Tokyo, Japan) in the presence of 5% (v/v) dimethyl sulfoxide for 30 cycles at 94 °C for 30 s, 54 or 50 °C for 42 s, and 68 °C for 4 min. The amplified cDNA fragment of *DS-epi1* or *DS-epi2* was subcloned into a pGEM®-T Easy vector (Promega, Madison, WI) and sequenced in a 377 DNA sequencer (Applied Biosystems, Carlsbad, CA) according to the manufacturer's instructions.

*In situ hybridization*

Brains were quickly removed from ddY mice at P7, P14, P21, and 7W, and frozen in powdered dry ice. Consecutive brain sections were cut 16-μm thick with a Cryostat CM3050S (Leica Microsystems, Wetzlar, Germany) at OPEN FACILITY, Hokkaido University Sousei

Hall, then thaw-mounted onto 3-aminopropyltriethoxysilane-procoated glass slides (Matsunami, Osaka, Japan), and stored at -80 °C prior to use.

$^{35}$S-Labeled riboprobes were transcribed using the MAXIscript®SP6/T7 kit (Ambion, Austin, TX) with uridine 5'-α[$^{35}$S]thiotriphosphate (~46.2 TBq/mmol) (PerkinElmer Life and Analytical Sciences, Waltham, MA) and *in situ* hybridization with $^{35}$S-labeled riboprobes was performed as described previously (Mitsunaga et al. 2006).

To identify *DS-epi2*-expressing cells in brain, a microautoradiographic analysis was performed. After hybridization with $^{35}$S-labeled riboprobes, the slides were dipped in an emulsion (NTB, Kodak, Rochester, NY) following the instructions of the manufacturer. Subsequently, the slides were exposed for 6 weeks at 4 °C in a light-tight box, and then they were developed with D-19 (Kodak). For microscope observation, the slides were counterstained with cresyl violet (Sigma, St. Louis, MO).

*Quantification of the expression of DS-epi1 and DS-epi2 in the brain by real-time PCR*

Brains were separated into four parts; the olfactory bulb, cerebrum/midbrain, cerebellum, and pons/medulla oblongata, and used individually for the experiments. Total RNA was extracted from the brain samples using an RNA isolation kit, illustra RNAspin Midi (GE Healthcare, Buckinghamshire, UK). Each cDNA was synthesized from ~1 μg of the total RNA using Moloney murine leukemia virus-reverse transcriptase (Promega) and an oligo(dT)$_{16}$ primer

(Hokkaido System Science, Sapporo, Japan). The primer sequences used were as follows: *DS-epi1* (302 bp), F 5'- TGG CAG CGC AGC CTA GTT G-3' and R 5'-ATA GGC CTC CTG AAG GTA CCC T-3'; *DS-epi2* (148 bp), F 5'-GAG CTT CTG GAT GTA TGG AG-3' and R 5'- CTG AAC CAG GGA GTG AGG T-3'; glyceraldehyde-3-phosphate dehydrogenase (*G3pdh*) (205 bp), F 5'-CAT CTG AGG GCC CAC TG-3' and R 5'-GAG GCC ATG TAG GCC ATG A-3'. Quantitative real-time PCR was performed using a Brilliant®II SYBER® Green QPCR master mix in Mx3005P Real Time QPCR (Agilent Technologies, Santa Clara, CA) at OPEN FACILITY, Hokkaido University Sousei Hall. The levels of *DS-epi1* and *DS-epi2* mRNA were normalized to that of the transcript of *G3pdh*.

*Extraction of GAGs from various regions of the mouse brain at different stages of postnatal development*

The olfactory bulb, cerebrum/midbrain, cerebellum, and pons/medulla oblongata of ddY mice at P7, P14, P21, and 7W were dehydrated and delipidated by homogenization in ice-cold acetone, and dried in a desiccator. The number of mice used was 20, 20, 20 and 10, respectively. Approximately 20-800 mg of the dried material was recovered, and GAGs were extracted as described previously (Nandini et al. 2005). The thalamus and cerebral cortex were also dissected from 5 mice at 7W for the GAG analysis. The recovery of GAGs was determined with a carbazole reaction to measure uronic acids colorimetrically (Bitter and

Muir 1962).

*Analysis of the disaccharide composition of CS/DS*

The disaccharide composition of CS/DS in the GAG-peptide preparations from brain samples was determined as follows. The GAG-peptide preparations were dissolved in water and an aliquot (0.1-0.4 % of starting materials) was treated with CSase ABC (Yamagata et al. 1968) (10 mIU) or a mixture of CSases AC-I (Yamagata et al. 1968) and AC-II (Hiyama and Okada 1975) (1 and 5 mIU, respectively) in a total volume of 20 μl of 50 mM Tris-HCl buffer, pH 7.3, at 37 °C for 1 h. The enzyme solutions were dried and subjected to derivatization with a fluorophore 2AB as described previously (Kinoshita and Sugahara 1999). After the removal of excess 2AB reagent by extraction with chloroform, the resultant 2AB derivatives of unsaturated disaccharides were analyzed by anion-exchange HPLC on an amine-bound silica PA03 column (4.6 x 250 mm, YMC Corp., Kyoto, Japan) with a linear gradient of $NaH_2PO_4$ from 16 to 540 mM over 60 min at a flow rate of 1 ml/min. Identification and quantification of the disaccharides were achieved by comparison with the positions and fluorescence intensity of CS-derived authentic unsaturated disaccharides; ΔO, ΔC, ΔA, ΔD, ΔB, and ΔE. The amount of IdoA-containing disaccharides was calculated as follows: the total amount of disaccharides released by CSase ABC minus the amount released by a mixture of CSases AC-I and AC-II.

**Funding**

This work was supported in part by Grants-in-aid for Scientific Research B (20390019) (to K.S.), and the Future Drug Discovery and Medical Care Innovation Program (K.S.) of the Ministry of Education, Culture, Sports, Science, and Technology of Japan (MEXT). M.M. and A.M. were supported by grants from the Swedish Science Research Council.

**Footnote**

[4]Present address: Department of Pharmacodynamics, Meiji Pharmaceutical University, Kiyose, Tokyo 204-8588, Japan

**Abbreviations**

2AB, 2-aminobenzamide; CS, chondroitin sulfate; CSase, chondroitinase; DS, dermatan sulfate; DS-epi, dermatan sulfate epimerase; GAG, glycosaminoglycan; GalNAc, *N*-acetyl-D-galactosamine; GlcA, D-glucuronic acid; GlcNAc, *N*-acetyl-D-glucosamine; ΔHexA, 4,5-unsaturated hexuronic acid or 4-deoxy-α-L-*threo*-hex-4-enepyranosyluronic acid; HPLC, high performance liquid chromatography; IdoA, L-iduronic acid; PG, proteoglycan

A, GlcAβ1-3GalNAc(4-*O*-sulfate); iA, IdoAα1-3GalNAc(4-*O*-sulfate);

B, GlcA(2-*O*-sulfate)β1-3GalNAc(4-*O*-sulfate);

iB, IdoA(2-*O*-sulfate)α1-3GalNAc(4-*O*-sulfate); C, GlcAβ1-3GalNAc(6-*O*-sulfate);

iC, IdoAα1-3GalNAc(6-*O*-sulfate); D, GlcA(2-*O*-sulfate)β1-3GalNAc(6-*O*-sulfate);

iD, IdoA(2-*O*-sulfate)α1-3GalNAc(6-*O*-sulfate); E, GlcAβ1-3GalNAc(4,6-*O*-disulfate);

iE, IdoAα1-3GalNAc(4,6-*O*-disulfate); O, GlcAβ1-3GalNAc; iO, IdoAα1-3GalNAc;

F, forward; R, reverse; RT, reverse transcription; P, postnatal day; 2S, 2-*O*-sulfate;

4S, 4-*O*-sulfate; 6S, 6-*O*-sulfate

**References**

Bao X, Muramatsu T, Sugahara K. 2005. Demonstration of the pleiotrophin-binding oligosaccharide sequences isolated from chondroitin sulfate/dermatan sulfate hybrid chains of embryonic pig brains. *J Biol Chem*. 280:35318-35328.

Bao X, Nishimura S, Mikami T, Yamada S, Itoh N, Sugahara K. 2004. Chondroitin sulfate/dermatan sulfate hybrid chains from embryonic pig brain, which contain a higher proportion of L-iduronic acid than those from adult pig brain, exhibit neuritogenic and growth factor binding activities. *J Biol Chem*. 279:9765-9776.

Basappa, Murugan S, Sugahara KN, Lee CM, ten Dam GB, van Kuppevelt TH, Miyasaka M, Yamada S, Sugahara K. 2009. Involvement of chondroitin sulfate E in the liver tumor focal formation of murine osteosarcoma cells. *Glycobiology*. 19:735-742.

Bitter T, Muir HM. 1962. A modified uronic acid carbazole reaction. *Anal Biochem*. 4:330-334.

Casu B, Petitou M, Provasoli M, Sinaÿ P. 1988. Conformational flexibility: a new concept for explaining binding and biological properties of iduronic acid-containing glycosaminoglycans. *Trends Biochem Sci*. 13:221-225.

Clement AM, Nadanaka S, Masayama K, Mandl C, Sugahara K, Faissner A. 1998. The DSD-1 carbohydrate epitope depends on sulfation, correlates with chondroitin sulfate D motifs, and is sufficient to promote neurite outgrowth. *J Biol Chem*. 273:28444-28453.

Clement AM, Sugahara K, Faissner A. 1999. Chondroitin sulfate E promotes neurite outgrowth of rat embryonic day 18 hippocampal neurons. *Neurosci Lett*. 269:125-128.

Cöster L, Malmström A, Sjöberg I, Fransson LÅ. 1975. The co-polymeric structure of pig skin dermatan sulphate: distribution of L-iduronic acid sulphate residues in co-polymeric chains. *Biochem J*. 145:379-389.

Dündar M, Müller T, Zhang Q, Pan J, Steinmann B, Vodopiutz J, Gruber R, Sonoda T, Krabichler B, Utermann G, Baenziger JU, Zhang L, Janecke AR. 2009. Loss of dermatan-4-sulfotransferase 1 function results in adducted thumb-clubfoot syndrome. *Am J Hum Genet*. 85:873-882.

Esko JD, Selleck SB. 2002. Order out of chaos: assembly of ligand binding sites in heparan sulfate. *Annu Rev Biochem*. 71:435-471.

Faissner A, Clement A, Lochter A, Streit A, Mandl C, Schachner M. 1994. Isolation of a

neural chondroitin sulfate proteoglycan with neurite outgrowth promoting properties. *J Cell Biol*. 126:783-799.

Ferro DR, Provasoli A, Ragazzi M, Casu B, Torri G, Bossennec V, Perly B, Sinaÿ P, Petitou M, Choay J. 1990. Conformer populations of L-iduronic acid residues in glycosaminoglycan sequences. *Carbohydr Res*. 195:157-167.

Fransson LÅ, Rodén L. 1967. Structure of dermatan sulfate: I. Degradation by testicular hyaluronidase. *J Biol Chem*. 242:4161-4169.

Goossens D, Van Gestel S, Claes S, De Rijk P, Souery D, Massat I, Van den Bossche D, Backhovens H, Mendlewicz J, Van Broeckhoven C, Del-Favero J. 2003. A novel CpG-associated brain-expressed candidate gene for chromosome 18q-linked bipolar disorder. *Mol Psychiatry*. 8:83-89.

Habuchi H, Yamagata T, Iwata H, Suzuki S. 1973. The occurrence of a wide variety of dermatan sulfate-chondroitin sulfate copolymers in fibrous cartilage. *J Biol Chem*. 248:6019-6028.

Hikino M, Mikami T, Faissner A, Vilela-Silva ACES, Pavão MSG, Sugahara K. 2003. Oversulfated dermatan sulfate exhibits neurite outgrowth-promoting activity toward embryonic mouse hippocampal neurons: implications of dermatan sulfate in

neuritogenesis in the brain. *J Biol Chem*. 278:43744-43754.

Hiyama K, Okada S. 1975. Crystallization and some properties of chondroitinase from *Arthrobacter aurescens*. *J Biol Chem*. 250:1824-1828.

Ishii M, Maeda N. 2008. Spatiotemporal expression of chondroitin sulfate sulfotransferases in the postnatal developing mouse cerebellum. *Glycobiology*. 18:602-614.

Izumikawa T, Koike T, Shiozawa S, Sugahara K, Tamura J, Kitagawa H. 2008. Identification of chondroitin sulfate glucuronyltransferase as chondroitin synthase-3 involved in chondroitin polymerization: chondroitin polymerization is achieved by multiple enzyme complexes consisting of chondroitin synthase family members. *J Biol Chem*. 283:11396-11406.

Izumikawa T, Uyama T, Okuura Y, Sugahara K, Kitagawa H. 2007. Involvement of chondroitin sulfate synthase-3 (chondroitin synthase-2) in chondroitin polymerization through its interaction with chondroitin synthase-1 or chondroitin-polymerizing factor. *Biochem J*. 403:545-552.

Kinoshita A, Sugahara K. 1999. Microanalysis of glycosaminoglycan-derived oligosaccharides labeled with a fluorophore 2-aminobenzamide by high-performance liquid chromatography: application to disaccharide composition analysis and

exosequencing of oligosaccharides. *Anal Biochem*. 269: 367-378.

Kitagawa H, Izumikawa T, Uyama T, Sugahara K. 2003. Molecular cloning of a chondroitin polymerizing factor that cooperates with chondroitin synthase for chondroitin polymerization. *J Biol Chem*. 278:23666-23671.

Kitagawa H, Tsutsumi K, Tone Y, Sugahara K. 1997. Developmental regulation of the sulfation profile of chondroitin sulfate chains in the chicken embryo brain. *J Biol Chem*. 272:31377-31381.

Kitagawa H, Uyama T, Sugahara K. 2001. Molecular cloning and expression of a human chondroitin synthase. *J Biol Chem.* 276:38721-38726.

Kobayashi M, Sugumaran G, Liu J, Shworak NW, Silbert JE, Rosenberg RD. 1999. Molecular cloning and characterization of a human uronyl 2-sulfotransferase that sulfates iduronyl and glucuronyl residues in dermatan/chondroitin sulfate. *J Biol Chem*. 274:10474-10480.

Kusche-Gullberg M, Kjellén L. 2003. Sulfotransferases in glycosaminoglycan biosynthesis. *Curr Opin Struct Biol*. 13:605-611.

Li F, Shetty AK, Sugahara K. 2007. Neuritogenic activity of chondroitin/dermatan sulfate hybrid chains of embryonic pig brain and their mimicry from shark liver:

involvement of the pleiotrophin and hepatocyte growth factor signaling pathways. *J Biol Chem*. 282:2956-2966.

Li F, ten Dam GB, Murugan S, Yamada S, Hashiguchi T, Mizumoto S, Oguri K, Okayama M, van Kuppevelt TH, Sugahara K. 2008. Involvement of highly sulfated chondroitin sulfate in the metastasis of the Lewis lung carcinoma cells. *J Biol Chem*. 283:34294-34304.

Li F, Nandini CD, Hattori T, Bao X, Murayama D, Nakamura T, Fukushima N, Sugahara K. 2010. Structure of pleiotrophin- and hepatocyte growth factor-binding sulfated hexasaccharide determined by biochemical and computational approaches. *J Biol Chem*. 285:27673-27685.

Linhardt RJ, Avci FY, Toida T, Kim YS, Cygler M. 2006. CS lyases: structure, activity, and applications in analysis and the treatment of diseases. In: Volpi N, editor. Chondroitin sulfate: structure, role and pharmacological activity. London (UK): Academic Press. p. 187-215.

Maccarana M, Kalamajski S, Kongsgaard M, Magnusson SP, Oldberg Å, Malmström A. 2009. Dermatan sulfate epimerase 1-deficient mice have reduced content and changed distribution of iduronic acids in dermatan sulfate and an altered collagen structure in skin. *Mol Cell Biol*. 29:5517-5528.

Maccarana M, Olander B, Malmström J, Tiedemann K, Aebersold R, Lindahl U, Li JP, Malmström A. 2006. Biosynthesis of dermatan sulfate: chondroitin-glucuronate C5-epimerase is identical to SART2. *J Biol Chem*. 281:11560-11568.

Maimone MM, Tollefsen DM. 1990. Structure of a dermatan sulfate hexasaccharide that binds to heparin cofactor II with high affinity. *J Biol Chem*. 265:18263-18271.

Malmström A. 1984. Biosynthesis of dermatan sulfate: II. Substrate specificity of the C-5 uronosyl epimerase. *J Biol Chem*. 259:161-165.

McCormick C, Duncan G, Goutsos KT, Tufaro F. 2000. The putative tumor suppressors EXT1 and EXT2 form a stable complex that accumulates in the Golgi apparatus and catalyzes the synthesis of heparan sulfate. *Proc Natl Acad Sci USA*. 97:668-673.

Michelacci YM, Dietrich CP. 1974. Isolation and partial characterization of an induced chondroitinase B from *Flavobacterium heparinum*. *Biochem Biophys Res Commun*. 56:973-980.

Mikami T, Mizumoto S, Kago N, Kitagawa H, Sugahara K. 2003. Specificities of three distinct human chondroitin/dermatan *N*-acetylgalactosamine 4-*O*-sulfotransferases demonstrated using partially desulfated dermatan sulfate as an acceptor: implication of differential roles in dermatan sulfate biosynthesis. *J Biol Chem*. 278:36115-36127.

Mitsunaga C, Mikami T, Mizumoto S, Fukuda J, Sugahara K. 2006. Chondroitin sulfate/dermatan sulfate hybrid chains in the development of cerebellum: spatiotemporal regulation of the expression of critical disulfated disaccharides by specific sulfotransferases. *J Biol Chem*. 281:18942-18952.

Miyake N, Kosho T, Mizumoto S, Furuichi T, Hatamochi A, Nagashima Y, Arai E, Takahashi K, Kawamura R, Wakui K, et al. 2010. Loss-of-function mutations of CHST14 in a new type of Ehlers-Danlos syndrome. *Hum Mutat*. 31:966-974.

Nadanaka S, Clement AM, Masayama K, Faissner A, Sugahara K. 1998. Characteristic hexasaccharide sequences in octasaccharides derived from shark cartilage chondroitin sulfate D with a neurite outgrowth promoting activity. *J Biol Chem*. 273:3296-3307.

Nakao M, Shichijo S, Imaizumi T, Inoue Y, Matsunaga K, Yamada A, Kikuchi M, Tsuda N, Ohta K, Takamori S, Yamana H, Fujita H, Itoh K. 2000. Identification of a gene coding for a new squamous cell carcinoma antigen recognized by the CTL. *J Immunol*. 164:2565-2574.

Nandini CD, Itoh N, Sugahara K. 2005. Novel 70-kDa chondroitin sulfate/dermatan sulfate hybrid chains with a unique heterogeneous sulfation pattern from shark skin, which exhibit neuritogenic activity and binding activities for growth factors and

neurotrophic factors. *J Biol Chem*. 280:4058-4069.

Nandini CD, Mikami T, Ohta M, Itoh N, Akiyama-Nambu F, Sugahara K. 2004. Structural and functional characterization of oversulfated chondroitin sulfate/dermatan sulfate hybrid chains from the notochord of hagfish: neuritogenic and binding activities for growth factors and neurotrophic factors. *J Biol Chem*. 279:50799-50809.

Ohtake S, Kimata K, Habuchi O. 2003. A unique nonreducing terminal modification of chondroitin sulfate by *N*-acetylgalactosamine 4-sulfate 6-*O*-sulfotransferase. *J Biol Chem*. 278:38443-38452.

Pacheco B, Maccarana M, Malmström A. 2009a. Dermatan 4-*O*-sulfotransferase 1 is pivotal in the formation of iduronic acid blocks in dermatan sulfate. *Glycobiology*. 19:1197-1203.

Pacheco B, Malmström A, Maccarana M. 2009b. Two dermatan sulfate epimerases form iduronic acid domains in dermatan sulfate. *J Biol Chem*. 284:9788-9795.

Penc SF, Pomahac B, Winkler T, Dorschner RA, Eriksson E, Herndon M, Gallo RL. 1998. Dermatan sulfate released after injury is a potent promoter of fibroblast growth factor-2 function. *J Biol Chem*. 273:28116-28121.

Petit E, Delattre C, Papy-Garcia D, Michaud P. 2006. Chondroitin sulfate lyases: applications

in analysis and glycobiology. In: Volpi N, editor. Chondroitin sulfate: structure, role and pharmacological activity. London (UK): Academic Press. p. 167-186.

Pinhal MAS, Smith B, Olson S, Aikawa J, Kimata K, Esko JD. 2001. Enzyme interactions in heparan sulfate biosynthesis: uronosyl 5-epimerase and 2-*O*-sulfotransferase interact *in vivo*. *Proc Natl Acad Sci USA*. 98:12984-12989.

Presto J, Thuveson M, Carlsson P, Busse M, Wilén M, Eriksson I, Kusche-Gullberg M, Kjellén L. 2008. Heparan sulfate biosynthesis enzymes EXT1 and EXT2 affect NDST1 expression and heparan sulfate sulfation. *Proc Natl Acad Sci USA*. 105:4751-4756.

Rodier PM. 1977. Correlations between prenatally-induced alterations in CNS cell populations and postnatal function. *Teratology*. 16:235-246.

Senay C, Lind T, Muguruma K, Tone Y, Kitagawa H, Sugahara K, Lidholt K, Lindahl U, Kusche-Gullberg M. 2000. The EXT1/EXT2 tumor suppressors: catalytic activities and role in heparan sulfate biosynthesis. *EMBO Rep*. 1:282-286.

Shors TJ. 2009. Saving new brain cells. *Sci Am*. 300:46-52, 54.

Sugahara K, Mikami T. 2007. Chondroitin/dermatan sulfate in the central nervous system. *Curr Opin Struct Biol*. 17: 536-545.

Thiele H, Sakano M, Kitagawa H, Sugahara K, Rajab A, Höhne W, Ritter H, Leschik G, Nürnberg P, Mundlos S. 2004. Loss of chondroitin 6-*O*-sulfotransferase-1 function results in severe human chondrodysplasia with progressive spinal involvement. *Proc Natl Acad Sci USA*. 101:10155-10160.

Trowbridge JM, Rudisill JA, Ron D, Gallo RL. 2002. Dermatan sulfate binds and potentiates activity of keratinocyte growth factor (FGF-7). *J Biol Chem*. 277:42815-42820.

Tuysuz B, Mizumoto S, Sugahara K, Çelebi A, Mundlos S, Turkmen S. 2009. Omani-type spondyloepiphyseal dysplasia with cardiac involvement caused by a missense mutation in *CHST3*. *Clin Genet*. 75:375-383.

van Roij MHH, Mizumoto S, Yamada S, Morgan T, Tan-Sindhunata MB, Meijers-Heijboer H, Verbeke JILM, Markie D, Sugahara K, Robertson SP. 2008. Spondyloepiphyseal dysplasia, Omani type: further definition of the phenotype. *Am J Med Genet A*. 146A:2376-2384.

Yamada S, Sugahara K. 2008. Potential therapeutic application of chondroitin sulfate/dermatan sulfate. *Curr Drug Discov Technol*. 5:289-301.

Yamagata T, Saito H, Habuchi O, Suzuki S. 1968. Purification and properties of bacterial chondroitinases and chondrosulfatases. *J Biol Chem*. 243:1523-1535.

Yoshida K, Arai M, Kohno Y, Maeyama K, Miyazono H, Kikuchi H, Morikawa K, Tawada A, Suzuki S. 1993. Activity of bacterial eliminases towards dermatan sulphates and dermatan sulphate proteoglycan. In: Scott JE, editor. Dermatan sulphate proteoglycans. London (UK): Portland Press. p. 55–70.

**Figure legends**

**Fig. 1.** Typical structure of disaccharide units found in CS and DS chains.

(**A**) The backbone of CS and DS chains is a linear polymer composed of repeating disaccharide units, [-4GlcAβ1-3GalNAcβ1-] and [-4IdoAα1-3GalNAcβ1-], respectively. These sugar residues can be modified by ester sulfate at various positions as indicated by the circled "S". DS is a stereoisomer of CS containing IdoA instead of GlcA, and CS and DS are often found as CS/DS hybrid chains (Sugahara and Mikami 2007). (**B**) Sequences of typical disaccharide units of CS (*left*) and DS (*right*). "i" in the DS disaccharide units represents IdoA. 2S, 4S, and 6S stand for 2-*O*-, 4-*O*-, and 6-*O*-sulfate, respectively.

**Fig. 2.** *In situ* hybridization of the *DS-epi1* and *DS-epi2* transcript in the mouse brain during postnatal development.

Consecutive sagittal sections from P7 (**A**), P14 (**B**), P21 (**C** and **E**), and 7W (**D**) mouse brains were hybridized with $^{35}$S-labeled antisense (**A**-**D**) or sense (**E**) cRNA probes for *DS-epi2*, and exposed to X-ray film for 6 weeks. Little signal for *DS-epi1* was detected in the sections of mice at various developmental stages. A representative autoradiogram from a P21 mouse is shown in panel *F*. Ob, olfactory bulb; Cb, cerebellum; Cx, cerebral cortex; Hi, hippocampus; Th, thalamus; Md, midbrain; Cpu, caudate putamen. Scale bar, 5 mm.

**Fig. 3.** Microautoradiographic detection of *DS-epi2* expression in the hippocampus.

Sagittal sections from 7W mouse brains were hybridized with $^{35}$S-labeled antisense (**A** and **C**) or sense (**B** and **D**) cRNA probes as described under the "Materials and methods". The signals (*dots*) were detected by microautoradiography. The granule cell layer of the dentate gyrus was counterstained with cresyl violet (*purple*). *DS-epi2* was expressed in the pyramidal cell layer composed of pyramidal cells (**A** and **C**). The regions enclosed by *squares* in panels **A** and **B** are shown at a higher magnification in the panels **C** and **D**, respectively. Scale bars, 0.1 mm. Py, pyramidal cell layer; GrDG, granule cell layer of the dentate gyrus.

**Fig. 4.** Quantitative real-time PCR analysis of the *DS-epi1* and *DS-epi2* transcripts in the mouse brain during postnatal development.

Total RNA was extracted from the olfactory bulb (**A**), cerebrum/midbrain (**B**), cerebellum (**C**), and pons/medulla oblongata (**D**) of a P7, P14, P21, or 7W mouse, and cDNA was synthesized by reverse transcriptase. Real-time PCR was conducted using the cDNAs, *Taq* polymerase, and SYBER Green. The expression of *DS-epi1* (*open circles*) and *DS-epi2* (*closed circles*) was individually normalized to that of glyceraldehyde-3-phosphate dehydrogenase (*G3pdh*). The assay was performed at least twice in duplicate, and representative results are shown. Values represent the mean ± S.D.

**Fig. 5.** Anion-exchange HPLC of disaccharides obtained from the digests of CS/DS derived from cerebrum/midbrain with CSase ABC or a mixture of CSases AC-I and AC-II.

The GAG-peptide fractions prepared from cerebrum/midbrain of P7 (**A** and **B**), P14 (**C** and **D**), P21 (**E** and **F**), and 7W (**G** and **H**) mice were treated with CSase ABC (**A**, **C**, **E**, and **G**) or a mixture of CSases AC-I and AC-II (**B**, **D**, **F**, and **H**). The individual digests were derivatized with a fluorophore (2AB) and analyzed by anion-exchange HPLC on an amine-bound silica PA03 column using a linear gradient of $NaH_2PO_4$, as indicated by the dashed line. The eluates were monitored by fluorescence intensity with excitation and emission wavelengths of 330 and 420 nm, respectively. The insets show magnified chromatograms (18-fold) around the elution positions of disulfated disaccharide units. The positions of the authentic 2AB-derivatized disaccharides are indicated by *numbered arrows*: 1, ΔO; 2, ΔC; 3, ΔA; 4, ΔD; 5, ΔB; 6, ΔE. The peaks marked by *asterisks* correspond to the 2AB-labeled ΔHexA-GlcNAc derived from hyaluronic acid, which was also digested by bacterial CSases (Linhardt et al. 2006; Petit et al. 2006).

**Fig. 6.** Composition of disaccharide units of CS/DS from various regions of mouse brain at different stages during postnatal development.

The CS/DS chains in the GAG-peptide preparations from olfactory bulb (**A** and **B**), cerebrum/midbrain (**C** and **D**), cerebellum (**E** and **F**), and pons/medulla oblongata (**G** and **H**)

of P7, P14, P21 and 7W mice were treated with CSase ABC or a mixture of CSases AC-I and AC-II. The digests were analyzed by anion-exchange HPLC (Fig. 5), and the amount of each disaccharide unit was quantified based on the peak areas of the disaccharides on chromatograms. The content of IdoA-containing disaccharides from DS was estimated as follows: the amount of disaccharides released by CSase ABC minus that released by a mixture of CSases AC-I and AC-II. The boxes in left panels (**A**, **C**, **E**, and **G**) show the major non- and monosulfated disaccharide units, iA, A, C, and O, and those in right panels (**B**, **D**, **F**, and **H**) show the minor disulfated units, iE, E, iB, B, iD, and D. iC and iO units were not detected.

A

Chondroitin sulfate (CS)

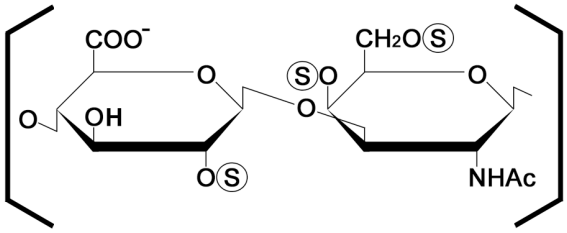


GlcA GalNAc

Dermatan sulfate (DS)

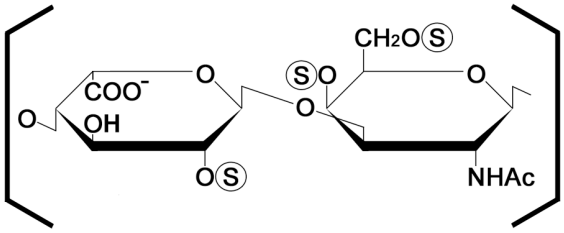


IdoA GalNAc

B

CS units

| Unit | Sequence |
|---|---|
| O unit | GlcA-GalNAc |
| A unit | GlcA-GalNAc(4S) |
| C unit | GlcA-GalNAc(6S) |
| B unit | GlcA(2S)-GalNAc(4S) |
| D unit | GlcA(2S)-GalNAc(6S) |
| E unit | GlcA-GalNAc(4S,6S) |
| T unit | GlcA(2S)-GalNAc(4S,6S) |

DS units

| Unit | Sequence |
|---|---|
| iO unit | IdoA-GalNAc |
| iA unit | IdoA-GalNAc(4S) |
| iC unit | IdoA-GalNAc(6S) |
| iB unit | IdoA(2S)-GalNAc(4S) |
| iD unit | IdoA(2S)-GalNAc(6S) |
| iE unit | IdoA-GalNAc(4S,6S) |
| iT unit | IdoA(2S)-GalNAc(4S,6S) |

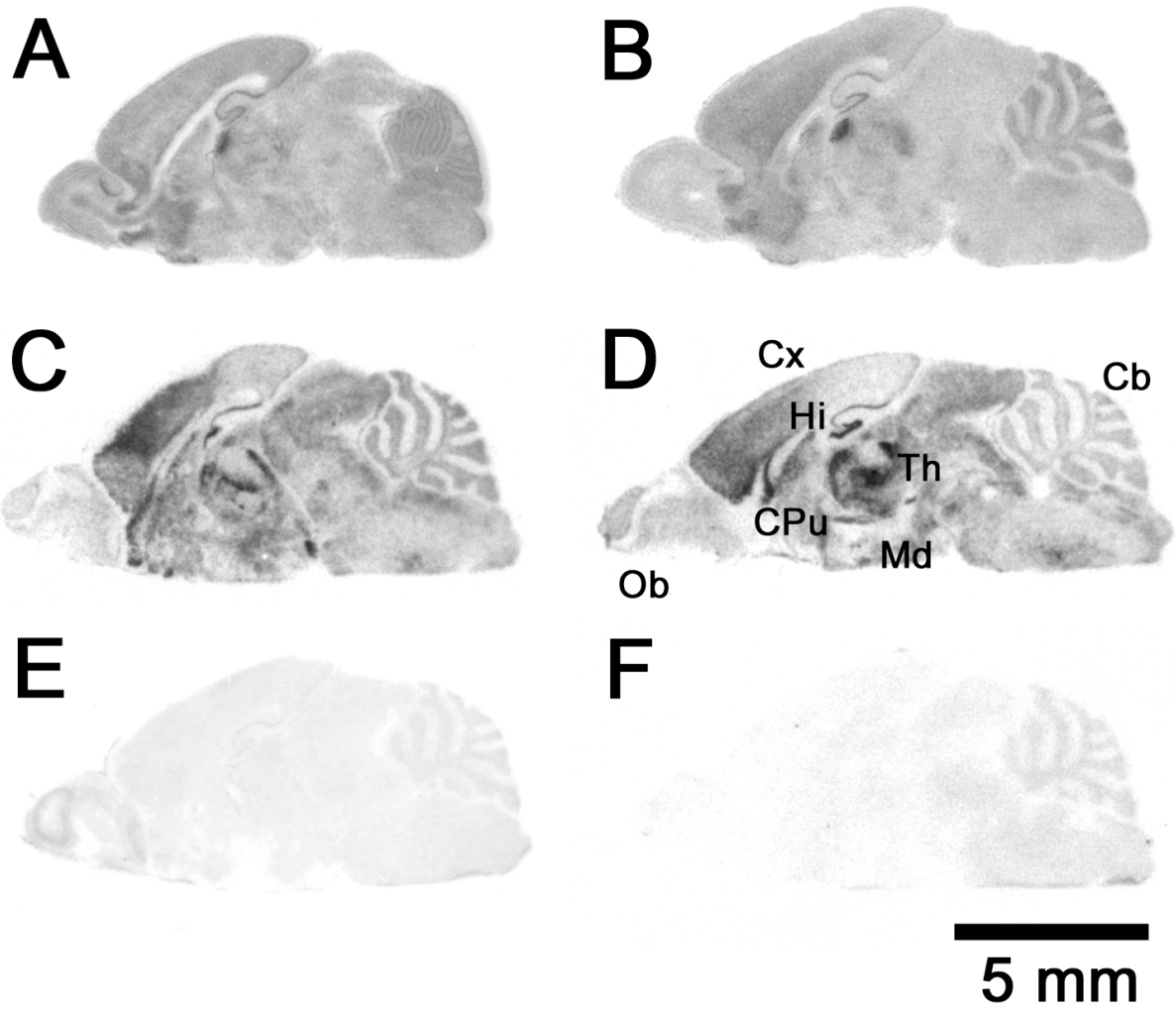
A
B
C
D
Cx
Cb
Hi
Th
CPu
Md
Ob
E
F
5 mm

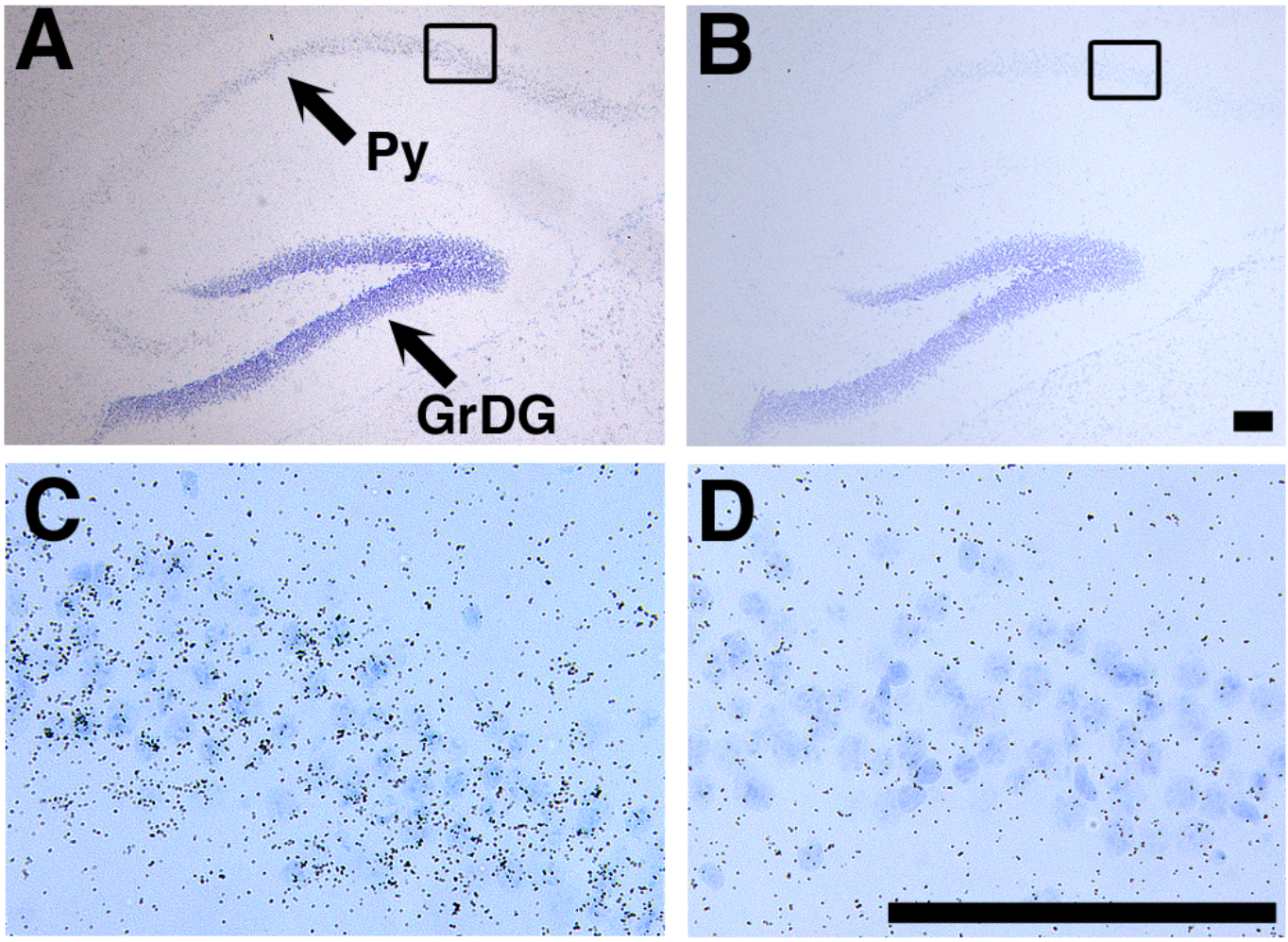
A
Py
GrDG
B
C
D

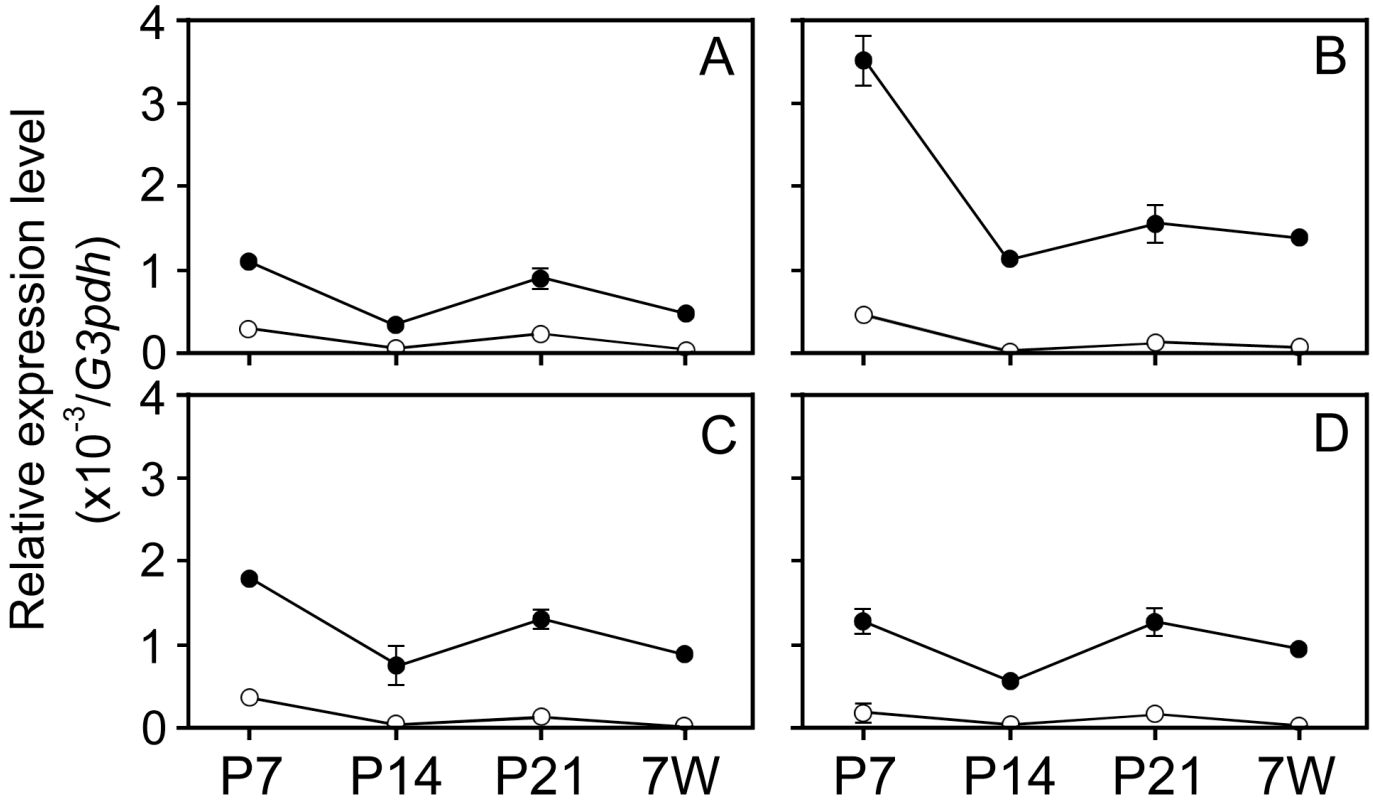
Relative expression level
(x10-3/G3pdh)
A
B
C
D
0
1
2
3
4
P7
P14
P21
7W

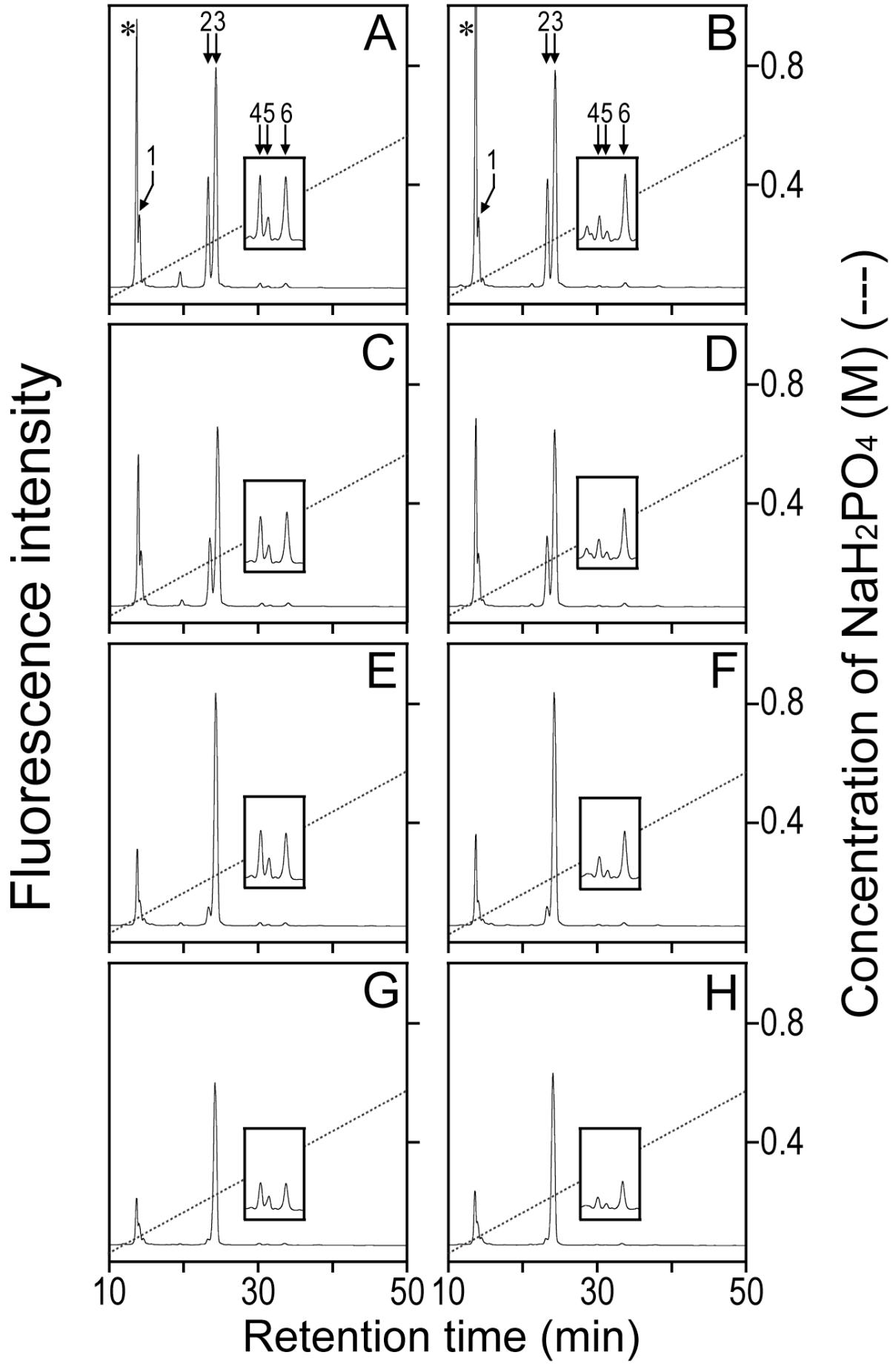
A
B
C
D
E
F
G
H
*
23
45 6
1
0.8
0.4
10
30
50
Retention time (min)
Fluorescence intensity
Concentration of NaH2PO4 (M) (---)

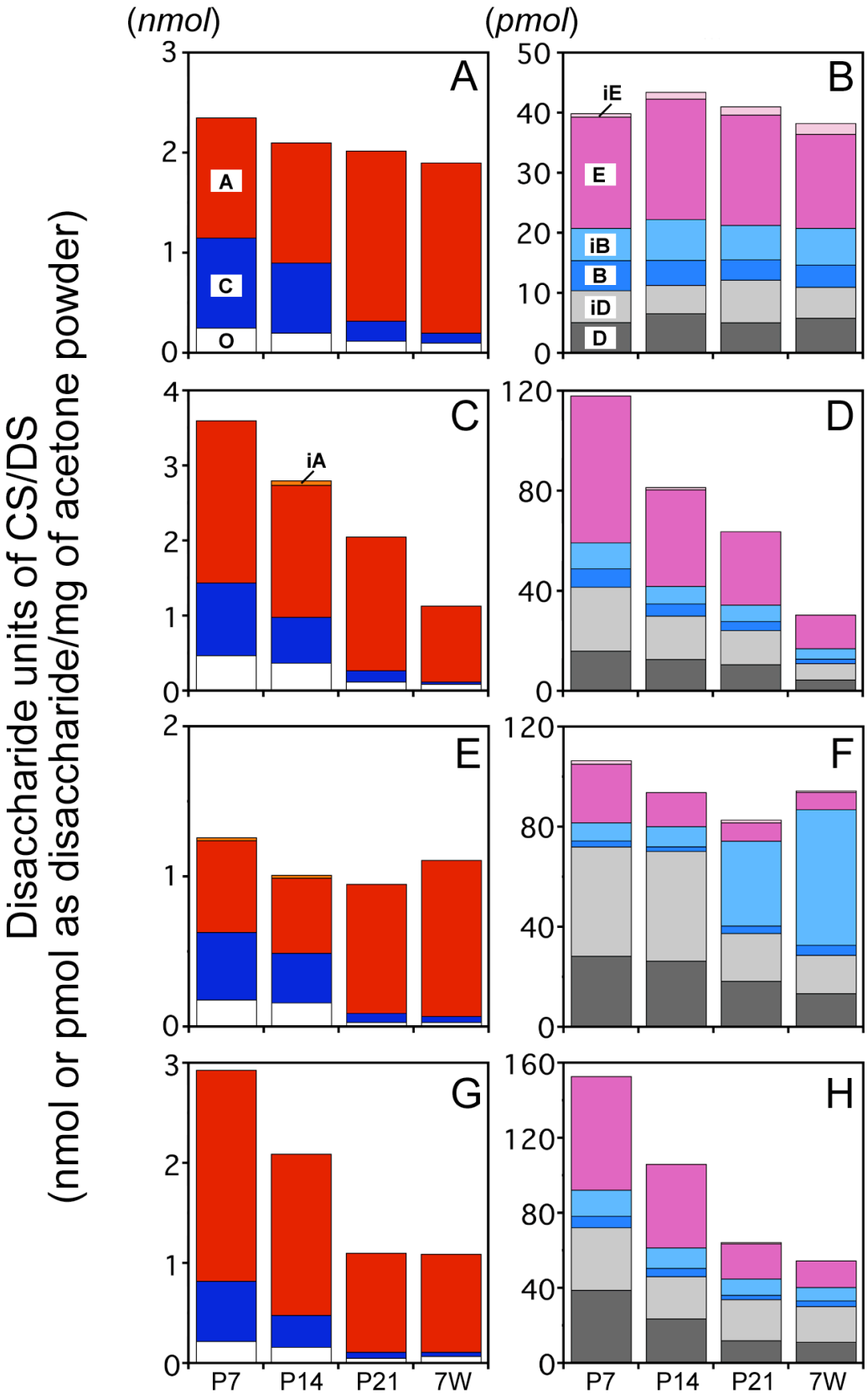
(nmol)
(pmol)
Disaccharide units of CS/DS
(nmol or pmol as disaccharide/mg of acetone powder)
A
B
C
D
E
F
G
H
A
C
O
iE
E
iB
B
iD
D
iA
P7
P14
P21
7W